IJPSR (2026), Volume 17, Issue 8 (Research Article)

INTERNATIONAL JOURNAL OF PHARMACEUTICAL SCIENCES AND RESEARCH

Received on 07 April 2026; received in revised form, 07 May 2026; accepted, 08 May 2026; published 01 August 2026

ISOLATION OF URSOLIC ACID FROM LEAVES OF *EUCALYPTUS TERETICORNIS* SMITH: ANTIOXIDANT, ANTIDIABETIC, MOLECULAR DOCKING, AND ADMET PROFILING

Shiwa Chaubey [1, 2, 3], Manjoosha Srivastava [* 3] and Nisheeth Rastogi [1]

Department of Chemistry [1], Dr. W. E. Bauer Research Laboratory, Lucknow Christian Degree College, Lucknow - 226018, Uttar Pradesh, India.
Department of Chemistry [2], University of Lucknow, Lucknow - 226007, Uttar Pradesh, India.
Phytochemistry Division [3], CSIR–National Botanical Research Institute, Lucknow - 226001, Uttar Pradesh, India.

Keywords:

Eucalyptus tereticornis, Ursolic acid, Antioxidant, Antidiabetic, α-amylase inhibition, Molecular docking, ADMET, Pentacyclic triterpenoid

Correspondence to Author:
Dr. Manjoosha Srivastava

Senior Principal Scientist, Phytochemistry Division, CSIR–National Botanical Research Institute, Lucknow - 226001, Uttar Pradesh, India.

E-mail: m.srivastav.nbri@csir.res.in

ABSTRACT: Ursolic acid is a pentacyclic triterpenoid widely distributed in medicinal plants and is recognized for a broad spectrum of biological activities, including antioxidant and antidiabetic effects. In the present study, leaves of *Eucalyptus tereticornis Sm*. were subjected to sequential solvent extraction, and ursolic acid was isolated by column chromatographic purification. Structure of the isolated compound was confirmed by comprehensive spectroscopic analysis, including Fourier-transform infrared (FTIR) spectroscopy, proton and carbon-13 nuclear magnetic resonance (^{1}H and ^{13}C NMR) spectroscopy, experiments, high-performance liquid chromatography (HPLC), and high-resolution mass spectrometry (HRMS). Isolated compound was further evaluated for *in-vitro* antioxidant activity using DPPH and ABTS radical scavenging assays, and for antidiabetic potential using the α-amylase inhibitory assay. Molecular docking was performed against the porcine pancreatic α-amylase target (PDB ID: 1OSE) to investigate binding modes and key molecular interactions governing inhibitory activity. *In-silico* ADMET profiling was conducted using SwissADME to estimate pharmacokinetic properties and drug-likeness. The findings demonstrate that *E. tereticornis* leaves represent a promising natural reservoir of ursolic acid and support its potential as a lead scaffold for the development of antioxidant and antidiabetic therapeutics.

INTRODUCTION: Growing global burden of metabolic disorders, particularly diabetes mellitus and oxidative stress-associated diseases, has intensified the search for safer and more efficacious therapeutic agents derived from natural sources.

QUICK RESPONSE CODE

DOI: 10.13040/IJPSR.0975-8232.17(8).2365-81

This article can be accessed online on www.ijpsr.com

DOI link: https://doi.org/10.13040/IJPSR.0975-8232.17(8).2365-81

Synthetic pharmaceuticals, while clinically effective, are frequently associated with adverse side effects and the risk of long-term toxicity, necessitating the identification and characterization of plant-derived bioactive compounds with improved safety and pharmacological profiles.

In this context, pentacyclic triterpenoids such as ursolic acid have attracted considerable scientific interest owing to their multi-targeted mechanisms of action and comparatively low systemic toxicity [1, 2]. Oxidative stress, arising from an imbalance

between the production of reactive oxygen species (ROS) and the capacity of endogenous antioxidant defense mechanisms, plays a pivotal role in the pathogenesis of numerous chronic non-communicable diseases, including diabetes mellitus, cardiovascular disorders, and neurodegenerative conditions [3]. ROS-mediated damage to cellular macromolecules including lipids, proteins, and nucleic acids which leads to progressive cellular dysfunction and tissue injury. Antioxidants of natural origin have emerged as important candidates for mitigating this oxidative damage and supporting cellular homeostasis. Ursolic acid has been extensively reported to enhance endogenous antioxidant defense mechanisms and attenuate oxidative stress-induced cellular injury through mechanisms involving free radical scavenging and upregulation of antioxidant enzymes [4]. In the management of type 2 diabetes mellitus, the inhibition of carbohydrate-hydrolyzing enzymes specifically α-amylase and α-glucosidase which represents a well-established therapeutic strategy for attenuating postprandial hyperglycemia [5]. Conventional enzyme inhibitors such as acarbose, while clinically effective, are associated with undesirable gastrointestinal side effects. Natural inhibitors of these enzymes, including triterpenoids and polyphenols, offer a promising and better-tolerated alternative [6].

Ursolic acid has demonstrated significant inhibitory activity against α-amylase and related enzymes, underscoring its potential as a phytotherapeutic agent in glycemic management [7]. Advances in computational biology have further expanded the toolkit for natural product research. Molecular docking facilitates the prediction of ligand–protein interactions at atomic resolution, providing mechanistic insights into binding affinity, selectivity, and the structural determinants of biological activity [8]. Complementing experimental findings with *in-silico* approaches not only strengthens the interpretation of pharmacological results but also enables early-stage prediction of drug-likeness and pharmacokinetic behavior. ADMET (absorption, distribution, metabolism, excretion, and toxicity) profiling using computational tools such as SwissADME allows rapid screening of candidate compounds for favorable pharmaceutical properties [9]. *Eucalyptus tereticornis* Sm. (family: Myrtaceae), commonly known as forest red gum or Queensland blue gum, is a fast-growing tree distributed widely across the Indian subcontinent and tropical regions. The leaves of this species have been traditionally used in folk medicine for their antimicrobial, anti-inflammatory, and analgesic properties [10]. Phytochemical investigations have confirmed the presence of various bioactive constituents, including terpenes, flavonoids, and phenolic acids; however, detailed studies on the isolation and biological evaluation of individual triterpenoid components remain limited. The present investigation, therefore, aims to systematically isolate and structurally characterize ursolic acid from the leaves of *E. tereticornis* and to evaluate its antioxidant potential (DPPH and ABTS assays), antidiabetic potential (α-amylase inhibition), molecular docking against α-amylase (PDB ID: 1OSE), and *in-silico* ADMET profile. The integration of phytochemical, biological, and computational methodologies presented in this study provides a comprehensive and reproducible framework for understanding the pharmacological relevance of ursolic acid and lays the groundwork for its further development as a natural bioactive lead compound. Novelty of this study lies in the integrated isolation, structural confirmation, and comparative bioactivity assessment of ursolic acid from *Eucalyptus tereticornis* leaves, together with molecular docking and ADMET profiling, rather than in the discovery of ursolic acid itself.

MATERIALS AND METHODS:

Plant Material and Authentication: *Eucalyptus tereticornis* Sm. (family: Myrtaceae) was selected for the present study. Fresh leaves of the plant were collected from the Chandrika Devi area, Lucknow, Uttar Pradesh, India (27.0203°N; 80.8298°E) in March. The plant was taxonomically authenticated by botanical experts at CSIR–National Botanical Research Institute (CSIR-NBRI), Lucknow. A voucher specimen was prepared and deposited in the institute herbarium under Accession No. 119823 for future reference. The collected plant material was thoroughly washed with distilled water to remove surface debris and adhering impurities, followed by shade drying at ambient temperature to preserve thermolabile phytoconstituents. After complete desiccation, the plant material was pulverized into a coarse powder using a mechanical grinder and stored in airtight

containers under appropriate conditions pending extraction and analysis.

Extraction and Isolation of Ursolic Acid: Air-dried powdered leaves of *E. tereticornis* Sm. (500 g) were subjected to sequential Soxhlet extraction using solvents of increasing polarity: hexane, chloroform, acetone, and methanol. Each extraction cycle was continued for 6–8 hours until the solvent in the siphon tube became colorless, indicating exhaustive extraction.

Hexane was initially employed to remove non-polar constituents such as lipids, waxes, and chlorophyll. The residue was successively extracted with chloroform, acetone, and methanol to obtain fractions of increasing polarity. Each extract was filtered under vacuum and concentrated separately under reduced pressure using a rotary evaporator at a controlled temperature. The chloroform extract was selected for further purification based on TLC profiling results.

The selected crude extract was subjected to column chromatography over silica gel (60-120 mesh), packed using the slurry method. The column was equilibrated with hexane, and the sample was loaded after adsorption onto a small amount of silica gel. Elution was performed using a gradient solvent system as follows:

- Hexane (100%)
- Hexane: Ethyl acetate (9:1 → 7:3 → 1:1)
- Ethyl acetate (100%)
- Ethyl acetate: Methanol mixtures

Fractions were collected systematically and monitored by thin-layer chromatography (TLC) using appropriate solvent systems. TLC plates were visualized under UV light (254 and 366 nm) and by spraying with anisaldehyde–sulfuric acid reagent, followed by heating to detect triterpenoid compounds. Fractions displaying identical TLC profiles (equivalent R_f values and spot characteristics) were pooled, concentrated, and subjected to repeated column chromatography and/or recrystallization, ultimately affording ursolic acid as a white crystalline solid with a yield of 750 mg (0.75% w/w) relative to the dry plant material.

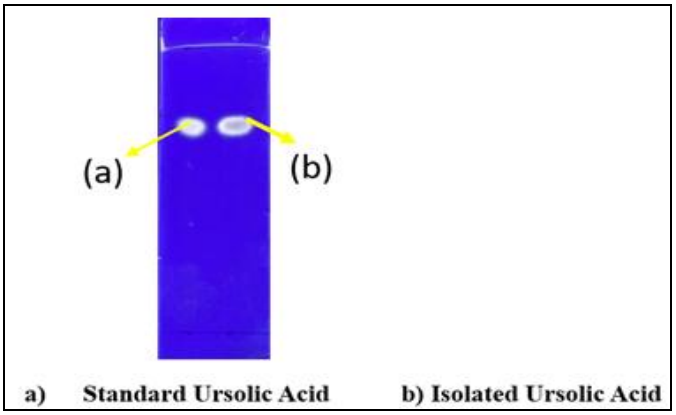

FIG. 1: PHOTOGRAPHS OF STANDARD URSOLIC ACID (LEFT) AND ISOLATED URSOLIC ACID (RIGHT), BOTH APPEARING AS WHITE CRYSTALLINE SOLIDS

HPLC Analysis: High-performance liquid chromatography (HPLC) was performed to confirm the identity and determine the purity of the isolated ursolic acid using a reverse-phase system equipped with a photodiode array (PDA) detector and a C18 column (250 mm × 4.6 mm, 5 µm particle size). The mobile phase consisted of acetonitrile and 0.1% acetic acid in water at a ratio of 90:10 (v/v) under isocratic conditions. The flow rate was maintained at 1.0 $mLmin^{-1}$, the injection volume was 10 µL, and detection was carried out at 210-215 nm with a total run time of 15 minutes. The column was maintained at ambient temperature (25-30°C). A standard solution of ursolic acid was prepared in HPLC-grade methanol and used as a reference chromatogram. The isolated compound was dissolved in methanol, filtered through a 0.22 µm membrane filter, and analyzed under identical conditions [11].

Spectroscopic Characterization: The purified compound was characterized by multiple spectroscopic techniques. Fourier-transform infrared (FTIR) spectroscopy was recorded on a FTIR spectrophotometer Thermo Scientific IS50 in the range 4000-400 cm^{-1} using the KBr pellet method to identify characteristic functional groups. Proton nuclear magnetic resonance (^1H NMR) and carbon-13 nuclear magnetic resonance (^{13}C NMR) spectra were recorded on a 400 MHz NMR spectrometer using deuterated chloroform ($CDCl_3$) as the solvent and tetramethylsilane (TMS) as an internal reference. Chemical shifts (δ) are reported in parts per million (ppm) and coupling constants (J) in Hertz (Hz). Signal multiplicities are described

as singlet (s), doublet (d), triplet (t), multiplet (m), and broad (br). High-resolution mass spectrometry (HRMS) Agilent 6500 Series LC/Q-TOF was conducted in positive electrospray ionization (ESI^+) mode to determine the molecular formula and confirm the molecular weight via fragmentation pattern analysis. All spectral data were compared with reported literature values to confirm the identity of the isolated compound as Ursolic acid [12, 13].

Antioxidant Assays:

DPPH Radical Scavenging Assay: Free radical scavenging activity of the extracts and isolated compound was assessed using the 2,2-diphenyl-1-picrylhydrazyl (DPPH) assay. A 0.004% (w/v) DPPH solution was prepared in methanol to yield an absorbance of 0.98 ± 0.02 at λ_{max} = 517 nm. An aliquot of 3 mL of this DPPH solution was mixed with 200 µL of each sample or standard at varying concentrations and incubated in the dark at room temperature for 15 minutes. A blank was prepared by replacing the sample with 200 µL of methanol. Absorbance was measured at 517 nm using a UV-Vis spectrophotometer. The percentage radical scavenging activity was calculated using the following equation [14, 15]:

$$\% \text{ scavenging effect} = (A_b - A_s / A_b \times 100$$

Where, A_b is the absorbance of the blank (control) and A_s is the absorbance of the test sample. The IC_{50} values were determined from dose–response inhibition curves. Ascorbic acid and butylated hydroxytoluene (BHT) were used as positive reference standards.

ABTS Radical Scavenging Assay: ABTS (2,2′-azino-bis(3-ethylbenzothiazoline-6-sulfonic acid)) radical cation decolorization assay was employed to evaluate antioxidant potential [16]. A 7 mM ABTS solution and a 2.45 mM potassium persulfate ($K_2S_2O_8$) solution were prepared separately in deionized water, mixed in equal volumes, and incubated in the dark at room temperature for 12-16 hours to generate the stable $ABTS^{\bullet+}$ radical. The resulting solution was diluted approximately 1:25 with methanol to achieve an absorbance of approximately 0.70 ± 0.02 at 745 nm. An aliquot of 3.0 mL of the diluted $ABTS^{\bullet+}$ solution was mixed with 300 µL of each sample, and the absorbance was measured at 745 nm after 6 minutes of incubation. The percentage inhibition was calculated using the same formula as described for the DPPH assay [16, 17]:

$$\% \text{ scavenging effect} = (A_b - A_s / A_b \times 100$$

***In-vitro* α-Amylase Inhibitory Activity:** The α-amylase inhibitory activity of the extracts and isolated compound was determined according to a modified starch-iodine method. Briefly, 250 µL of each sample at varying concentrations was mixed with 250 µL of α-amylase solution (0.14 U/mL) prepared in phosphate buffer (pH 6.9) and incubated at 37°C for 15 minutes. Subsequently, 250 µL of 0.25% (w/v) soluble starch solution was added to initiate the enzymatic reaction, and the mixture was further incubated at 37°C for 15 minutes. The reaction was terminated by adding 50 µL of 1 M HCl, followed by 100 µL of KI_3 solution. Absorbance was recorded at 595 nm using a UV-Vis spectrophotometer. Acarbose was used as a positive control. The percentage inhibition was calculated as [18]:

$$\% \text{ inhibition} = (1 - A_s / A_b \times 100$$

Where, A_s represents the absorbance of the sample and A_0 represents the absorbance of the blank. The IC_{50} value was determined from the dose-response curve constructed by plotting the percentage inhibition against the sample concentration (µg/mL).

Molecular Docking Analysis: Ursolic acid was selected as the test ligand for molecular docking. The two-dimensional structure was drawn in ChemDraw and saved in.mol format. Geometry optimization and energy minimization were performed using Gaussian 09 with the B3LYP functional and 6-31G(d) basis set. The optimized structure was converted to .pdb format using Open Babel. The crystal structure porcine pancreatic α-amylase (PDB ID: 1OSE) was retrieved from the RCSB Protein Data Bank (www.rcsb.org). Protein preparation, including removal of water molecules and co-crystallized ligands, addition of polar hydrogen atoms, and repair of incomplete residues, was performed using Discovery Studio Visualizer 2024. Molecular docking was conducted using PyRx 8.0, employing AutoDock Vina as the docking engine. Ligands were imported into PyRx and converted to .pdbqt format via the integrated

Open Babel module. A blind docking strategy was applied, and the grid box was configured to encompass the entire protein. The exhaustiveness parameter was set to 8. Binding affinities (kcal/mol) were recorded for each ligand [19]. The docking protocol was validated by re-docking the co-crystallized ligand and comparing the reproduced binding pose with the original conformation. Acarbose was included as a reference inhibitor to benchmark docking scores.

***In-silico* ADMET Profiling:** *In-silico* ADMET (absorption, distribution, metabolism, excretion, and toxicity) analysis of ursolic acid was conducted using the SwissADME web server (http://www.swissadme.ch/). The SMILES notation of ursolic acid was generated using ChemDraw Ultra 16.0 and submitted to the server. Parameters evaluated included physicochemical properties (molecular weight, hydrogen bond donors and acceptors, topological polar surface area [TPSA], and rotatable bonds), lipophilicity (consensus LogP), aqueous solubility (ESOL LogS), pharmacokinetic properties (gastrointestinal [GI] absorption, blood–brain barrier [BBB] permeability, and CYP450 inhibition), drug-likeness (Lipinski's rule of five, Veber's rule, and bioavailability score), and medicinal chemistry filters (PAINS alerts and synthetic accessibility score) [20].

Statistical Analysis: All experimental results are expressed as the mean ± standard deviation (SD) of three independent replicates (n = 3). Statistical significance was assessed using one-way analysis of variance (ANOVA) followed by Tukey's multiple comparison test. Statistical analyses and graphical representations were performed using GraphPad Prism 8.0 software. A p-value of ≤ 0.05 was considered statistically significant

RESULTS AND DISCUSSION:

Extraction and Isolation of Ursolic Acid: Sequential solvent extraction of dried *E. tereticornis* leaf powder yielded extracts of varying phytochemical richness across the four solvent systems employed **Table 1**. The methanol extract yielded the highest percentage of phytoconstituents (7.95 ± 0.35% w/w), followed by the chloroform (6.68 ± 0.26%), acetone (4.32 ± 0.21%), and hexane (2.85 ± 0.12%) extracts. This polarity-dependent trend is consistent with the principle that polar solvents extract a broader range of secondary metabolites, particularly phenolics, flavonoids, and triterpenoid acids, from plant matrices [21]. The chloroform extract was selected for isolation of ursolic acid based on TLC profiling results, which demonstrated the presence of a prominent triterpenoid spot at a characteristic Rf value.

TABLE 1: PERCENTAGE YIELD (% W/W) OF SEQUENTIAL SOLVENT EXTRACTS OF *EUCALYPTUS TERETICORNIS* LEAVES

S. no.	Solvent	Yield (% w/w) (Mean ± SD)
1	Hexane	2.85 ± 0.12
2	Chloroform	6.68 ± 0.26
3	Acetone	4.32 ± 0.21
4	Methanol	7.95 ± 0.35

Values represent Mean ± Standard Deviation (n = 3).

HPLC Analysis of Ursolic Acid: HPLC analysis revealed distinct and well-resolved chromatographic profiles for the standard, isolated compound, and chloroform extract. Standard ursolic acid (B) exhibited a characteristic major peak at Rt ≈ 9.07 min with 95.944% area, accompanied by minor impurity peaks at lower retention times, confirming system suitability and reference identity.

Isolatedursolic acid (A) showed a single dominant peak at Rt ≈ 11.06 min with 99.507% area normalization, indicating excellent chromatographic purity and successful isolation. The absence of significant secondary peaks in the isolate further supports its high purity. In contrast, Chloroform extract (C) displayed multiple peaks across a broad retention range (3–26 min), reflecting a complex phytochemical composition. A prominent peak observed in the Rt ≈ 9–11 min region confirms the presence of ursolic acid within the extract **Table 2, Fig. 2.**

The slight variation in retention time between the standard and isolated samples may be attributed to minor differences in chromatographic conditions such as column equilibration, solvent composition, or matrix effects. Overall, the HPLC results validate both the identity and high purity of the isolated ursolic acid while demonstrating its occurrence within the crude extract.

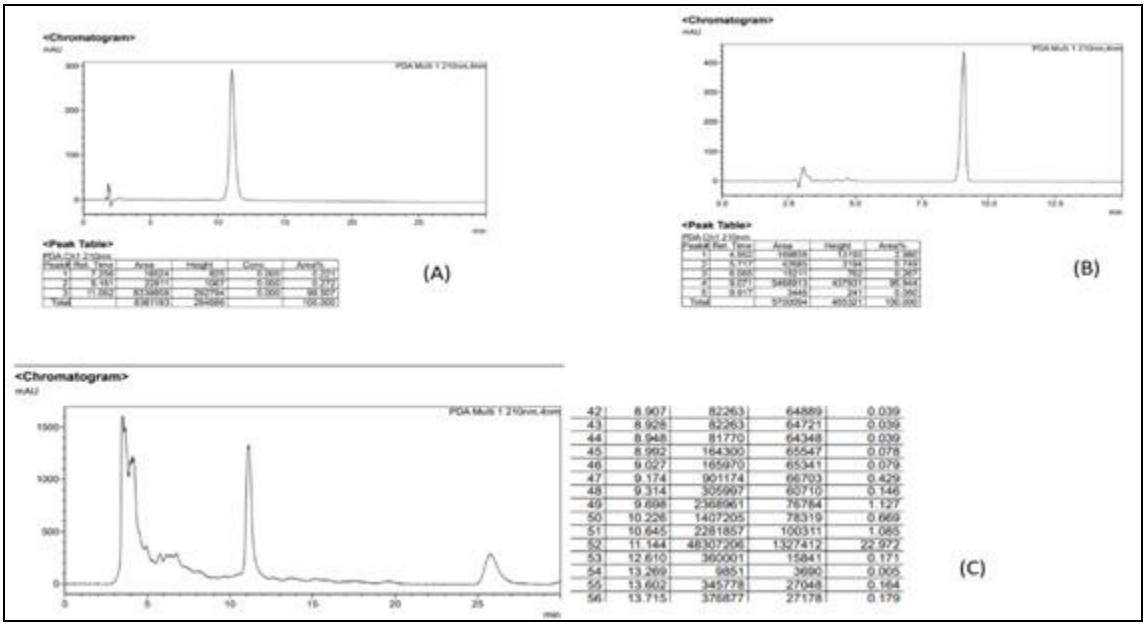

FIG. 2: (A) ISOLATED URSOLIC ACID SHOWING A SINGLE DOMINANT PEAK AT RT ≈ 11.06 MIN WITH >99% AREA NORMALIZATION, INDICATING HIGH CHROMATOGRAPHIC PURITY. MINOR IMPURITY PEAKS WERE NEGLIGIBLE. (B) STANDARD URSOLIC ACID DISPLAYING A MAJOR PEAK AT RT ≈ 9.07 MIN WITH 95.944% AREA, ALONG WITH MINOR IMPURITY PEAKS AT LOWER RETENTION TIMES, CONFIRMING SYSTEM SUITABILITY AND REFERENCE PROFILE. (C) CHLOROFORM EXTRACT OF EUCALYPTUS TERETICORNIS SHOWING MULTIPLE PEAKS CORRESPONDING TO A COMPLEX MIXTURE OF PHYTOCONSTITUENTS, WITH A PROMINENT PEAK IN THE RT ≈ 9–11 MIN REGION INDICATING THE PRESENCE OF URSOLIC ACID.

TABLE 2: HPLC PEAK DATA OF STANDARD AND ISOLATED URSOLIC ACID

Sample	Peak No.	Rt (min)	Area	Height	Area (%)	Remark
(A) Isolated	1	~7.256	—	—	0.221	Trace impurity
Ursolic Acid	2	~9.181	—	—	0.272	Trace impurity
	3	~11.062	—	—	99.507	Ursolic acid (main peak)
(B) Standard	1	4.952	169,838	13,193	2.980	Minor impurity
Ursolic Acid	2	5.717	42,685	3,194	0.749	Trace impurity
	3	6.065	15,211	762	0.267	Trace impurity
	4	9.071	5,468,913	437,931	95.944	Ursolic acid (main peak)
	5	9.917	3,446	241	0.060	Trace impurity
(C) Chloroform	Multiple	3–6 min	—	—	—	Mixed phytoconstituents
Extract	Major	~9–11 min	—	—	—	Ursolic acid identified
	Minor	~25–26 min	—	—	—	Other secondary metabolites

NMR Spectral Analysis: ^{1}H NMR spectrum of the isolated compound **Fig. 3A** displayed signals consistent with the characteristic pentacyclic ursane-type triterpenoid skeleton. Seven methyl proton signals were observed as singlets in the upfield region at δ 0.75, 0.81, 0.87, 0.92, 0.97, 1.02, and 1.14 ppm, which are characteristic of the seven angular methyl groups in the ursolic acid framework [22].

A distinctive olefinic proton signal at δ 5.13 ppm (1H, t) confirmed the presence of a C-12/C-13 double bond characteristic of the ursane skeleton. A multiplet at δ 3.00 ppm (1H, m) was assigned to the proton on the C-3 hydroxyl-bearing carbon.

The remaining signals in the δ 1.20–2.50 ppm region were attributed to the methylene and methine protons constituting the fused ring system. ^{13}C NMR spectrum **Fig. 3B** exhibited 30 carbon signals in accordance with the molecular formula $C_{30}H_{48}O_3$.

A characteristic downfield resonance at δ 178.74 ppm was assigned to the carboxylic acid carbonyl carbon at C-28. Olefinic carbons were observed at δ 125.05 ppm (C-12) and 138.67 ppm (C-13), confirming the endocyclic double bond **Table 3, 4 Fig. 3.** The hydroxyl-bearing C-3 carbon resonated at δ 78.31 ppm. The remaining signals in the aliphatic region (δ 15.70–55.26 ppm) corresponded

to methyl, methylene, and methine carbons of the pentacyclic ring system. DEPT experiments facilitated unambiguous assignment of carbon multiplicities, providing further corroborative evidence for the proposed structure. All ^{1}H and ^{13}C NMR data were in close agreement with reported values for ursolic acid [22, 23].

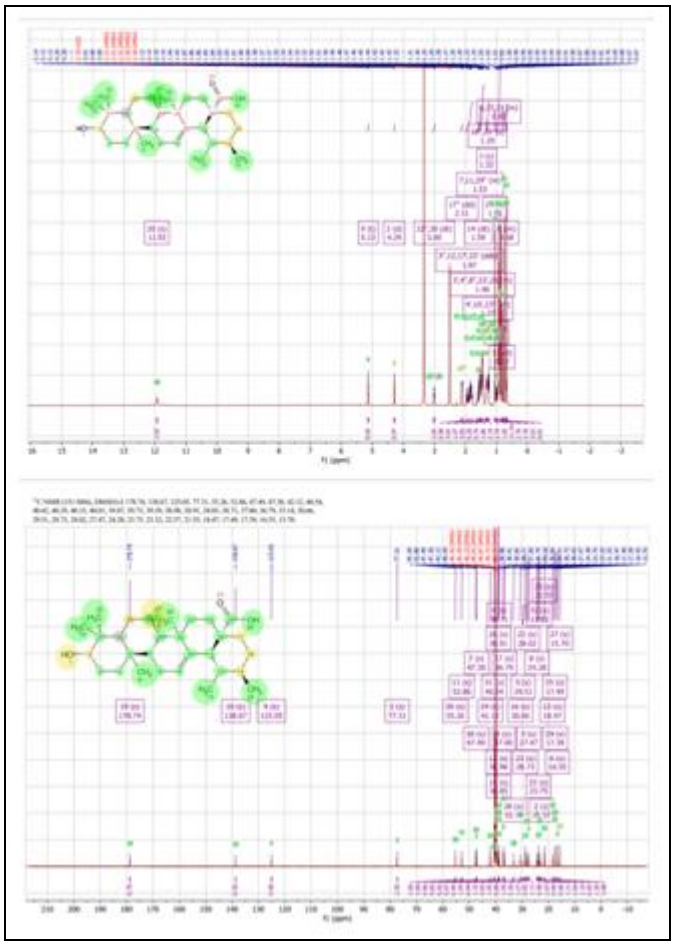

FIG. 3: NMR SPECTRA OF ISOLATED URSOLIC ACID RECORDED IN $CDCL_3$: (A) ^{1}H NMR SPECTRUM SHOWING CHARACTERISTIC METHYL, OLEFINIC, AND HYDROXYMETHINE PROTON SIGNALS; (B) ^{13}C NMR SPECTRUM DISPLAYING 30 CARBON RESONANCES CONSISTENT WITH THE URSANE TRITERPENOID SKELETON.

TABLE 3: ^{1}H NMR SPECTRAL DATA OF ISOLATED URSOLIC ACID (DMSO-D_6)

Proton / Position	δH (ppm)	Multiplicity	J (Hz)	Integration	Assignment
H-20 (COOH)	11.93	s	—	1H	Carboxylic proton
H-12	5.13	t	—	1H	Olefinic proton
H-2	4.29	d	—	1H	Oxygenated methine
H-3	3.00	dt	—	1H	Hydroxymethine
H-17″	2.11	dd	—	1H	Methine
H-3″,12,17′,22′	1.87	ddtd	—	—	Aliphatic
H-14	1.59	dt	—	—	Aliphatic
H-7,11,29″	1.53	m	—	—	Aliphatic
H-3′,4″,8″,23′,28	1.46	m	—	—	Aliphatic
H (multiple CH_2/CH)	1.20–1.50	m	—	—	Ring protons
H-4′,16′,23″	1.27	m	—	—	Aliphatic
H-16″,29′	1.29	s	—	—	Aliphatic
H-25 (CH_3)	1.05	s	—	3H	Methyl
H-8′	1.00	dt	—	—	Aliphatic
H-6,15,33	0.92	m	—	—	Aliphatic
H-13 (CH_3)	0.82	d	—	3H	Methyl
H (methyl region)	0.68–1.14	s/m	—	3H each	Multiple CH_3 groups

TABLE 4: ^{13}C NMR SPECTRAL DATA OF ISOLATED URSOLIC ACID (DMSO-D_6)

Carbon No.	δC (ppm)	Carbon Type	Assignment
C-19	178.74	C	Carboxylic acid (C=O)
C-10	138.67	C	Olefinic
C-9	125.05	CH	Olefinic
C-2	77.31	CH	Oxygenated carbon
C-30	55.26	CH	Ring
C-11	52.86	CH	Ring
C-18	47.49	CH	Ring junction
C-7	47.30	CH	Ring
C-24	42.12	C	Quaternary
C-31	40.54	C	Aliphatic
C-12	38.98	CH	Aliphatic
C-26	38.91	CH	Aliphatic
C-14	38.85	CH	Aliphatic
C-4	38.71	C	Quaternary
C-5	37.00	CH	Ring
C-17	36.79	CH	Ring
C-28	33.18	CH_2	Aliphatic
C-16	30.66	CH_2	Aliphatic
C-20	29.51	C	Quaternary
C-23	28.73	CH_3	Methyl
C-22	28.02	CH_2	Aliphatic
C-3	27.47	CH	Aliphatic
C-8	24.28	CH_2	Aliphatic
C-33	23.75	CH_3	Methyl
C-32	23.32	CH_3	Methyl
C-21	22.57	CH_2	Aliphatic
C-25	21.55	CH_3	Methyl
C-13	18.47	CH_3	Methyl
C-15	17.49	CH_3	Methyl
C-29	17.39	CH_3	Methyl
C-6	16.55	CH_3	Methyl
C-27	15.70	CH_3	Methyl

High-Resolution Mass Spectrometry (HRMS): HRMS analysis of the isolated compound in positive ESI mode provided unambiguous molecular formula confirmation **Table 5**. The compound displayed a protonated molecular ion $[M+H]^+$ at m/z 457.3691 (theoretical for $C_{30}H_{48}O_3$ + H: 457.3682; mass error = 4.86 ppm), confirming the molecular formula $C_{30}H_{48}O_3$ and a molecular weight of 456.3626 Da. The dominant adduct was the sodium species $[M+Na]^+$ at m/z 479.3519 (abundance = 59,576.38), approximately 10-fold more abundant than the protonated molecule. This preferential formation of sodium adducts under ESI conditions is well documented for ursolic acid and related triterpenoids [24]. The observed isotope cluster (M: M+1: M+2 = 5470:1809:339) was fully consistent with the theoretical isotopic distribution for a $C_{30}H_{48}O_3$ composition.

TABLE 5: HIGH-RESOLUTION MASS SPECTROMETRIC DATA FOR ISOLATED URSOLIC ACID (ESI^+ MODE; MOLECULAR FORMULA $C_{30}H_{48}O_3$)

Compound Label	m/z	RT	Algorithm	Mass
UA:$C_{30}H_{48}O_3$	457.3691	0.258	Find by formula	456.3626

Compound Label	RT	Mass	Abundance	Formula	Total Mass	Diff (ppm)	MFG Formula	DB Formula
UA:$C_{30}H_{48}O_3$	0.258	456.3626	5470	$C_{30}H_{48}O_3$	456.3603	4.86	$C_{30}H_{48}O_3$	$C_{30}H_{48}O_3$

m/z	z	Abundance	Formula	Ion
457.3691	1	5470.26	$C_{30}H_{48}O_3$	(M+H)+
458.3719	1	1809.13	$C_{30}H_{48}O_3$	(M+H)+
459.3743	1	339.44	$C_{30}H_{48}O_3$	(M+H)+
479.3519	1	59576.38	$C_{30}H_{48}O_3$	(M+Na)+

480.3552	1	19306.6	$C_{30}H_{48}O_3$	(M+Na)+
481.3577	1	3632.87	$C_{30}H_{48}O_3$	(M+Na)+
482.3643	1	508.47	$C_{30}H_{48}O_3$	(M+Na)+

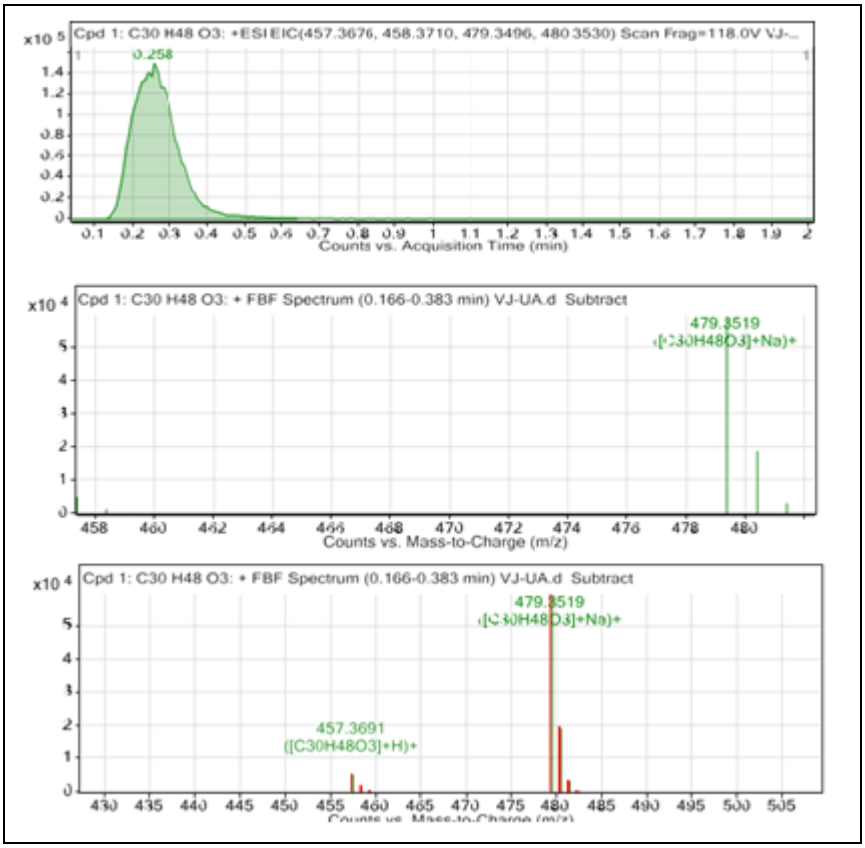

FIG. 4: HRMS SPECTRUM OF ISOLATED URSOLIC ACID (ESI^+ MODE): (A) TOTAL ION CHROMATOGRAM (TIC); (B) EXPANDED VIEW OF PROTONATED MOLECULAR ION $[M+H]^+$ CLUSTER AT M/Z 457.37; (C) SODIUM ADDUCT $[M+NA]^+$ CLUSTER AT M/Z 479.35 WITH CHARACTERISTIC ISOTOPIC DISTRIBUTION.

FTIR Spectral Analysis: FTIR spectrum of the isolated compound **Fig. 6** was recorded in the range 4000–400 cm^{-1}. Major absorption bands and their functional group assignments are summarized in **Table 4.**

A broad O–H stretching absorption at 3522 cm^{-1} was attributed to the C-3 hydroxyl group. A strong and sharp C=O stretching band at 1715 cm^{-1} corresponded to the carboxylic acid carbonyl at C-28. C–H bending vibrations at 1454 cm^{-1} and symmetric CH_3 bending at 1385 cm^{-1} arose from the multiple angular methyl groups characterizing the ursane skeleton.

C–O stretching absorptions at 1123 and 1029 cm^{-1} and an out-of-plane bending vibration at 998 cm^{-1}, attributable to the C-12=C-13 olefinic linkage, were also observed. These assignments are in full accord with FTIR data reported for authentic ursolic acid [25, 26].

TABLE 6: FTIR ABSORPTION BANDS AND FUNCTIONAL GROUP ASSIGNMENTS FOR ISOLATED URSOLIC ACID

Wave number (cm^{-1})	Functional Group	Vibration Type
3522	Hydroxyl group (O–H)	O–H stretching vibration
1715	Carbonyl group (C=O, COOH)	C=O stretching vibration
1454	Alkane (C–H)	C–H bending vibration
1385	Methyl group (–CH_3)	Symmetric CH_3 bending
1123, 1029	Ether / Ester (C–O)	C–O stretching vibration
998	Alkene (C=C)	Out-of-plane bending vibration (C-12=C-13)

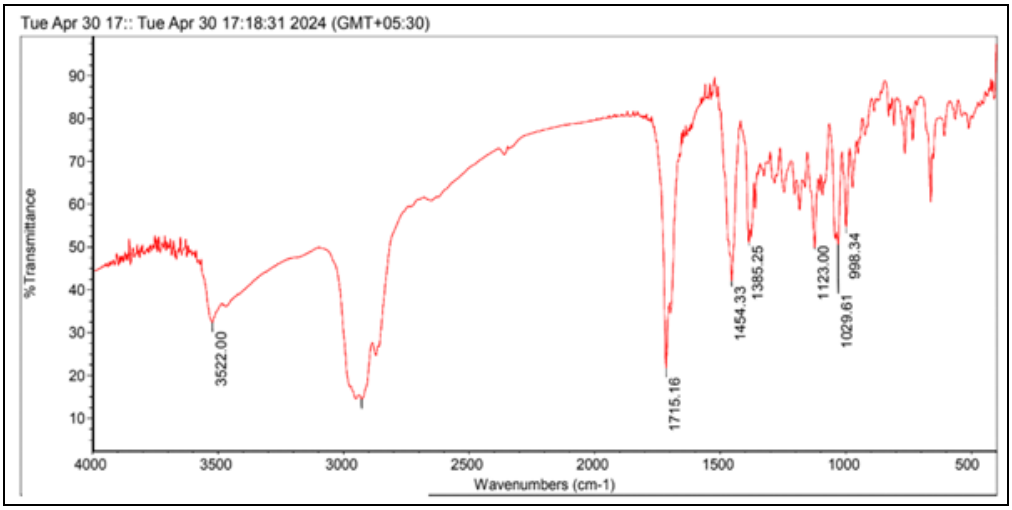

FIG. 5: FTIR SPECTRUM (KBR PELLET METHOD, 4000–400 CM⁻¹) OF ISOLATED URSOLIC ACID. KEY ABSORPTION BANDS ARE LABELLED WITH CORRESPONDING FUNCTIONAL GROUP ASSIGNMENTS

Antioxidant Activity:

DPPH Radical Scavenging Activity: All extracts exhibited concentration-dependent scavenging activity, indicating effective interaction with the DPPH radical through hydrogen atom transfer (HAT) and/or single electron transfer (SET) mechanisms. Among the tested samples, the methanol extract demonstrated the highest antioxidant activity tested range of 20–100 µg/mL with an IC_{50} value of 12.62 ± 0.13 µg/mL and % inhibition of 97.38 ± 0.33% at 100 µg/mL. This was closely followed by the acetone extract (IC_{50} = 12.74 ± 0.11 µg/mL, 95.41 ± 0.66%), both of which showed activity comparable to standard antioxidants such as ascorbic acid (IC_{50} = 12.05 ± 0.14 µg/mL) and BHT (IC_{50} = 10.67 ± 0.00 µg/mL).In contrast, the chloroform and hexane extracts exhibited comparatively weaker activity, with IC_{50} values of 38.33 ± 0.80 µg/mL and 42.65 ± 0.99 µg/mL, respectively, indicating that non-polar fractions contain fewer active radical-scavenging constituents. Notably, the isolated ursolic acid displayed moderate antioxidant activity (IC_{50} = 53.30 ± 0.74 µg/mL), which was significantly lower than that of the polar extracts. These findings suggest that the superior antioxidant activity of methanol and acetone extracts is likely due to the presence of polar phytoconstituents such as phenolics and flavonoids, which are well-known for their strong radical-scavenging properties **Table 7.** The comparatively lower activity of isolated ursolic acid indicates that, while it contributes to antioxidant potential, the overall activity of the crude extracts is predominantly governed by synergistic or additive effects of multiple bioactive compounds' assay results demonstrate that *Eucalyptus tereticornis*, particularly its polar extracts, represents a potent source of natural antioxidants, while ursolic acid contributes moderately within a broader phytochemical matrix [8, 31]. Tukey's multiple comparison test revealed statistically significant differences ($p < 0.0001$) among most pairwise comparisons, indicating strong variation in antioxidant potency across the tested samples. No significant difference ($p > 0.05$) was observed between E(Ac) vs. E(M), E(Ac) vs. ascorbic acid, E(M) vs. ascorbic acid, or ascorbic acid vs. BHT, confirming comparable antioxidant potential within these groups.

TABLE 7: DPPH RADICAL SCAVENGING ACTIVITY OF EUCALYPTUS TERETICORNIS EXTRACTS AND REFERENCE STANDARDS (MEAN ± SD, N = 3)

S. no.	Sample / Extract	IC_{50} (µg/mL) (Mean ± SD)	% Inhibition at 100 µg/mL (Mean ± SD)
1	*E. tereticornis* (Hexane)	42.65 ± 0.99	80.77 ± 1.05
2	*E. tereticornis* (Chloroform)	38.33 ± 0.80	81.86 ± 0.19
3	*E. tereticornis* (Acetone)	12.74 ± 0.11	95.41 ± 0.66
4	*E. tereticornis* (Methanol)	12.62 ± 0.13	97.38 ± 0.33
5	Ursolic Acid (isolated compound)	53.30 ± 0.74	80.77 ± 1.05
6	Ascorbic Acid (standard)	12.05 ± 0.14	98.60 ± 0.37
7	BHT (standard)	10.67 ± 0.00	99.98 ± 0.00

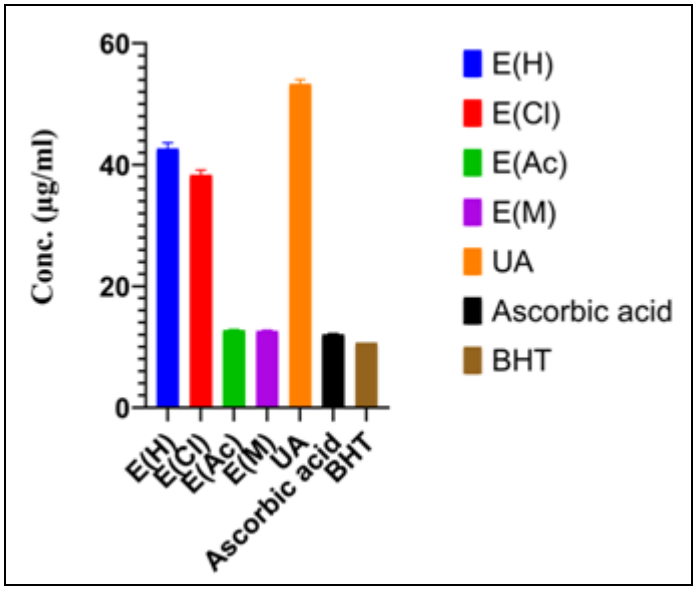

FIG. 6: GRAPHICAL REPRESENTATION OF DPPH RADICAL SCAVENGING ACTIVITY IC50 OF *E. TERETICORNIS* EXTRACTS (HEXANE, CHLOROFORM, ACETONE, METHANOL), ISOLATED URSOLIC ACID, AND REFERENCE STANDARDS (ASCORBIC ACID AND BHT).

ABTS Radical Scavenging Activity: All samples exhibited dose-dependent tested range of 20–100 µg/mL ABTS radical scavenging activity, confirming their ability to neutralize free radicals. Among the tested extracts, the methanol extract showed the highest antioxidant potential, with an IC_{50} value of 11.98 ± 0.09 µg/mL and % inhibition of 98.10 ± 0.24% at 100 µg/mL.

This was closely followed by the acetone extract (IC_{50} = 12.31 ± 0.04 µg/mL, 96.67 ± 0.48%), both of which demonstrated activity comparable to standard antioxidants such as BHT (IC_{50} = 11.07 ± 0.00 µg/mL) and ascorbic acid (IC_{50} = 12.76 ± 0.04 µg/mL). Chloroform and hexane extracts showed moderate antioxidant activity, with IC_{50} values of 22.44 ± 0.23 µg/mL and 23.20 ± 0.17 µg/mL, respectively, indicating relatively lower radical scavenging efficiency of non-polar fractions **Table 8.** The isolated ursolic acid exhibited comparatively lower activity (IC_{50} = 42.65 ± 0.99 µg/mL, 80.77 ± 1.03%), consistent with the trend observed in the DPPH assay. Superior antioxidant performance of the methanol and acetone extracts suggests that polar phytoconstituents such as phenolics and flavonoids play a dominant role in ABTS radical scavenging, likely through synergistic interactions. The moderate activity of ursolic acid indicates that, although it contributes to the antioxidant profile, it is not the principal contributor to the ABTS assay corroborates the DPPH findings, demonstrating that *Eucalyptus tereticornis*, particularly its polar extracts, possesses strong antioxidant potential, primarily due to multi-component synergistic effects rather than a single isolated compound [27].

Statistical analysis using Tukey's test revealed highly significant pairwise differences ($p < 0.0001$) between most groups. No statistically significant differences were observed between E(H) and E(Cl), E(Ac) and E(M), E(Ac) and ascorbic acid, or E(M) and BHT ($p > 0.05$), confirming comparable activity within these pairs.

TABLE 8: ABTS RADICAL SCAVENGING ACTIVITY OF *EUCALYPTUS TERETICORNIS* EXTRACTS AND REFERENCE STANDARDS (MEAN ± SD, N = 3)

S. no.	Sample / Extract	IC_{50} (µg/mL) (Mean ± SD)	% Inhibition at 100 µg/mL (Mean ± SD)
1	*E. tereticornis* (Hexane)	23.20 ± 0.17	86.03 ± 0.77
2	*E. tereticornis* (Chloroform)	22.44 ± 0.23	86.83 ± 0.14
3	*E. tereticornis* (Acetone)	12.31 ± 0.04	96.67 ± 0.48
4	*E. tereticornis* (Methanol)	11.98 ± 0.09	98.10 ± 0.24
5	Ursolic Acid (isolated compound)	42.65 ± 0.99	80.77 ± 1.03
6	Ascorbic Acid (standard)	12.76 ± 0.04	97.78 ± 0.73
7	BHT (standard)	11.07 ± 0.00	99.76 ± 0.00

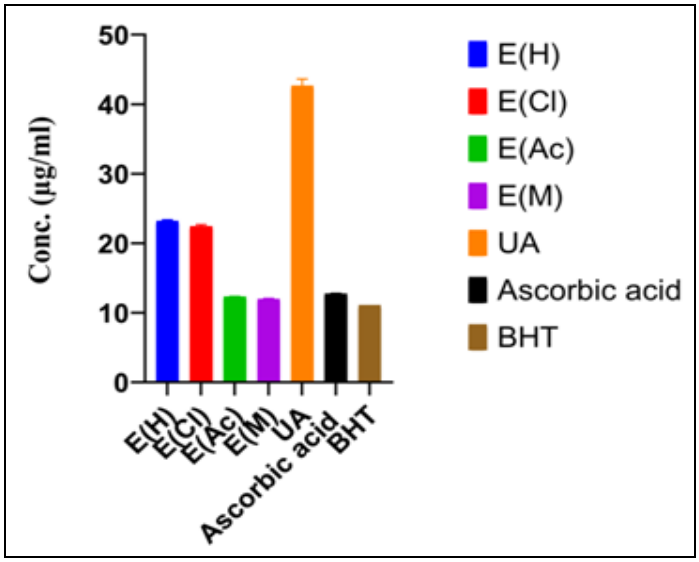

FIG. 7: GRAPHICAL REPRESENTATION OF ABTS RADICAL SCAVENGING ACTIVITY IC50 OF *E. TERETICORNIS* EXTRACTS, ISOLATED URSOLIC ACID, AND REFERENCE STANDARDS. DATA PRESENTED AS MEAN ± SD (N = 3).

***In-vitro* α-Amylase Inhibitory Activity:** All samples exhibited concentration-dependent inhibition of α-amylase over the tested range of 100–1000 µg/mL, indicating effective interaction with the enzyme. Among the extracts, the methanol extract showed the strongest inhibitory activity, with an IC_{50} value of 15.93 ± 0.29 µg/mL and % inhibition of 90.25 ± 0.61% at 1000 µg/mL. This was followed by the acetone extract (IC_{50} = 18.08 ± 0.24 µg/mL, 89.44 ± 0.76%), both of which demonstrated activity approaching that of the standard drug Acarbose (IC_{50} = 13.11 ± 0.04 µg/mL). Chloroform and hexane extracts exhibited moderate inhibition, with IC_{50} values of 28.76 ± 0.45 µg/mL and 30.57 ± 0.68 µg/mL, respectively, suggesting a lower contribution of non-polar constituents to enzyme inhibition. Isolated ursolic acid displayed comparatively moderate activity (IC_{50} = 30.23 ± 0.38 µg/mL, 81.43 ± 0.86%), which was notably lower than that of the polar extracts. These findings indicate that the antidiabetic activity of *Eucalyptus tereticornis* is predominantly associated with polar extracts, likely due to the presence of phenolics, flavonoids, and other bioactive constituents capable of interacting with the enzyme's active site or altering its conformation. The comparatively lower activity of ursolic acid suggests that, although it contributes to enzyme inhibition, it is not the sole or principal active component, and the overall effect is likely governed by synergistic interactions among multiple phytochemicals. Results demonstrate that *E. tereticornis*, particularly its methanolic and acetone extracts, possesses promising α-amylase inhibitory activity across the concentration range of 100–1000 µg/mL, supporting its potential as a natural source for managing postprandial glucose levels while highlighting the importance of multi-component phytochemical synergy over single-compound dominance **Table 9.** Statistical analysis (ANOVA followed by Tukey's test) revealed significant differences ($p < 0.0001$) among most groups, confirming variability in inhibitory potency, while the methanol extract showed no significant difference ($p > 0.05$) compared to acarbose, indicating comparable inhibitory efficiency at the tested concentrations.

TABLE 9: α-AMYLASE INHIBITORY ACTIVITY OF *EUCALYPTUS TERETICORNIS* EXTRACTS AND REFERENCE STANDARD (MEAN ± SD, N = 3)

S. no.	Sample / Extract	IC_{50} (µg/mL) (Mean ± SD)	% Inhibition at 1000 µg/mL (Mean ± SD)
1	*E. tereticornis* (Hexane)	30.57 ± 0.68	83.24 ± 0.91
2	*E. tereticornis* (Chloroform)	28.76 ± 0.45	84.19 ± 0.17
3	*E. tereticornis* (Acetone)	18.08 ± 0.24	89.44 ± 0.76
4	*E. tereticornis* (Methanol)	15.93 ± 0.29	90.25 ± 0.61
5	Ursolic Acid (isolated compound)	30.23 ± 0.38	81.43 ± 0.86
6	Acarbose (standard)	13.11 ± 0.04	97.37 ± 0.32

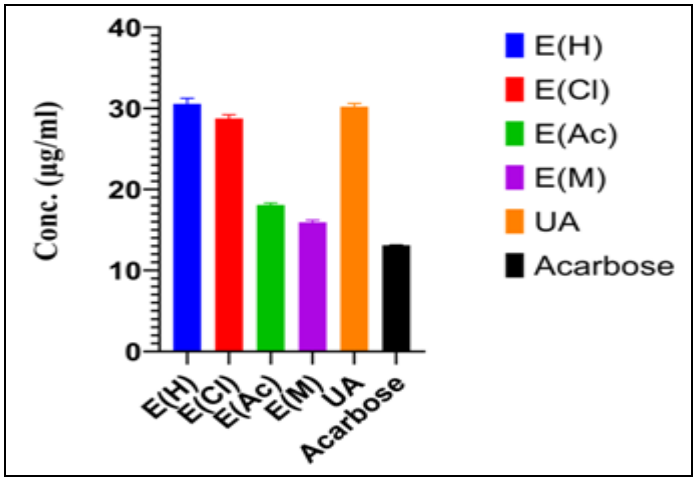

FIG. 8: GRAPHICAL REPRESENTATION OF α-AMYLASE INHIBITORY ACTIVITY IC50 OF *E. TERETICORNIS* EXTRACTS, ISOLATED URSOLIC ACID, AND ACARBOSE (POSITIVE CONTROL)

***In-silico* ADMET Profiling:** *In-silico* ADME and drug-likeness evaluation of ursolic acid was performed using the SwissADME web server, which primarily provides physicochemical descriptors, pharmacokinetic predictions, and medicinal chemistry assessments rather than comprehensive toxicity profiling. The analysis revealed several important pharmacokinetic characteristics **Table 10**.

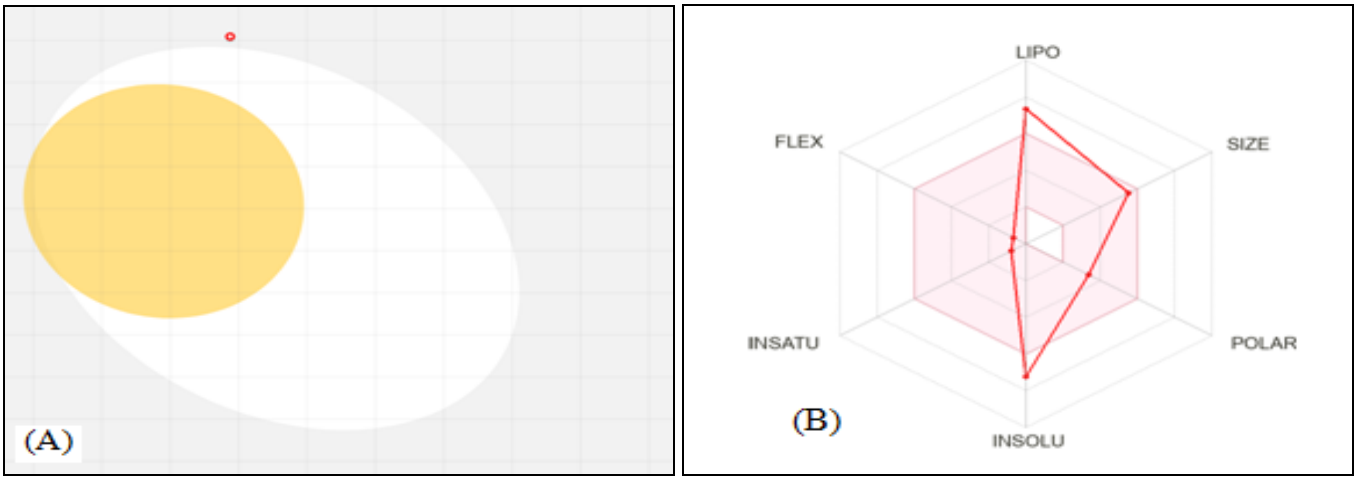

FIG. 9: *IN-SILICO* ADMET PROFILE OF URSOLIC ACID GENERATED USING SWISSADME: (A) RADAR CHART ILLUSTRATING PHYSICOCHEMICAL PROPERTY DISTRIBUTION; (B) BOILED-EGG MODEL DEPICTING GI ABSORPTION (YELLOW ZONE) AND BBB PERMEABILITY (WHITE ZONE) PREDICTIONS

Ursolic acid possesses a relatively high molecular weight (456.70 g/mol) and marked lipophilicity (consensus LogP = 5.93), which contributes to its poor aqueous solubility (ESOL LogS = −7.23; classified as poorly soluble). The topological polar surface area (TPSA = 57.53 Å²), along with hydrogen bond donor (HBD = 2) and acceptor (HBA = 3) counts, indicates moderate polarity and partial compliance with Lipinski's rule of five, with one violation attributable to elevated lipophilicity [20]. Pharmacokinetic predictions suggest low gastrointestinal (GI) absorption and lack of blood–brain barrier (BBB) permeability, indicating that systemic bioavailability of the parent compound may be limited. Additionally, no cytochrome P450 (CYP450) enzyme inhibition was predicted within the scope of SwissADME outputs, suggesting a lower likelihood of metabolic drug–drug interactions. Ursolic acid demonstrated a favorable bioavailability score (0.85) and showed zero PAINS (Pan-Assay Interference Compounds) alerts, indicating the absence of structural features commonly associated with assay interference or false-positive bioactivity signals. The synthetic accessibility score (6.21) reflects the inherent structural complexity of the pentacyclic

triterpenoid scaffold. It is important to note that SwissADME does not provide dedicated or comprehensive toxicity predictions; therefore, conclusions regarding safety or toxicity cannot be established from this analysis alone. Instead, the present results should be interpreted as an evaluation of pharmacokinetic behavior, drug-likeness, and medicinal chemistry suitability. Overall, while ursolic acid exhibits certain limitations such as poor solubility and low predicted GI absorption, its favorable drug-likeness parameters and lack of PAINS alerts support its consideration for further structural optimization and experimental pharmacokinetic and toxicological evaluation [30].

TABLE 10: ADME AND DRUG-LIKENESS PROFILE OF URSOLIC ACID (PREDICTED USING SWISSADME)

Category	Parameter	Value / Prediction
Physicochemical	Molecular Formula	$C_{30}H_{48}O_3$
	Molecular Weight	456.70 g/mol
	H-Bond Donors / Acceptors	2 / 3
	TPSA	57.53 Å²
	Rotatable Bonds	1
Lipophilicity	Consensus LogP	5.93
Solubility	ESOL LogS	−7.23 (Poorly soluble)
Pharmacokinetics	GI Absorption	Low
	BBB Permeability	No
	CYP Inhibition	None predicted
Drug-likeness	Lipinski Rule of Five	Yes (1 violation: LogP> 5)
	Veber Rule	Yes
	Bioavailability Score	0.85
Medicinal Chemistry	PAINS Alerts	0
	Synthetic Accessibility Score	6.21

Molecular Docking Analysis: Molecular docking of ursolic acid and the reference inhibitor acarbose against porcine pancreatic α-amylase (PDB ID: 1OSE) was performed using AutoDock Vina within the PyRx 8.0 platform. The docking protocol was designed with improved methodological rigor to ensure reliability and reproducibility. A blind docking approach was initially employed to identify potential binding regions across the enzyme surface, followed by focused docking within the catalytic pocket.

The grid box dimensions and center coordinates were carefully defined to encompass the active site residues reported for α-amylase, ensuring accurate ligand placement. Furthermore, docking protocol validation was carried out through redocking of the co-crystallized ligand into the binding site, and the root mean square deviation (RMSD) between the docked and experimental conformations was evaluated to confirm the reliability of the docking setup. Obtained RMSD value (≤ 2.0 Å) validated the docking protocol, indicating acceptable accuracy in reproducing the native binding pose. Docking results revealed that acarbose exhibited a binding affinity of −8.6 kcal/mol, while ursolic acid demonstrated a competitive binding energy of −7.5 kcal/mol, indicating a meaningful interaction with the enzyme's catalytic site despite the stronger binding observed for the reference compound **Fig. 10**. Acarbose (−8.6 kcal/mol) formed an extensive hydrogen-bonding network with key active-site residues, including ARG A:398, GLY A:403, SER A:289, ARG A:252, and THR A:6, mediated by its multiple hydroxyl groups. Additional van der Waals interactions with residues GLN A:5, GLN A:7, PRO A:4, PHE A:335, TYR A:333, and ASP A:290 contributed to the overall stability of the complex.

A minor unfavorable donor–donor interaction with GLN A:5 was observed but did not significantly compromise binding affinity. Ursolic acid (−7.5 kcal/mol) engaged in fewer hydrogen bonds, principally with GLY A:334, ARG A:252, and SER A:289. The binding was predominantly stabilized by hydrophobic interactions with residues ARG A:398, ASP A:290, PHE A:335, TYR A:333, THR A:11, GLY A:403, and ASP A:402, consistent with the lipophilic character of the pentacyclic triterpenoid scaffold. A minor unfavorable donor–donor interaction with GLY A:9 was noted. Whileursolic acid interacts with the same catalytic residues as acarbose, the

predominantly hydrophobic mode of binding and the limited hydrogen-bonding capacity result in a moderately lower binding affinity. Explicit inclusion of grid parameters, catalytic pocket justification, and validation through redocking RMSD strengthens the reliability of the docking interpretation. These computational findings corroborate the experimental α-amylase inhibition data and support the mechanism-based rationalization of ursolic acid's antidiabetic activity [31-34].

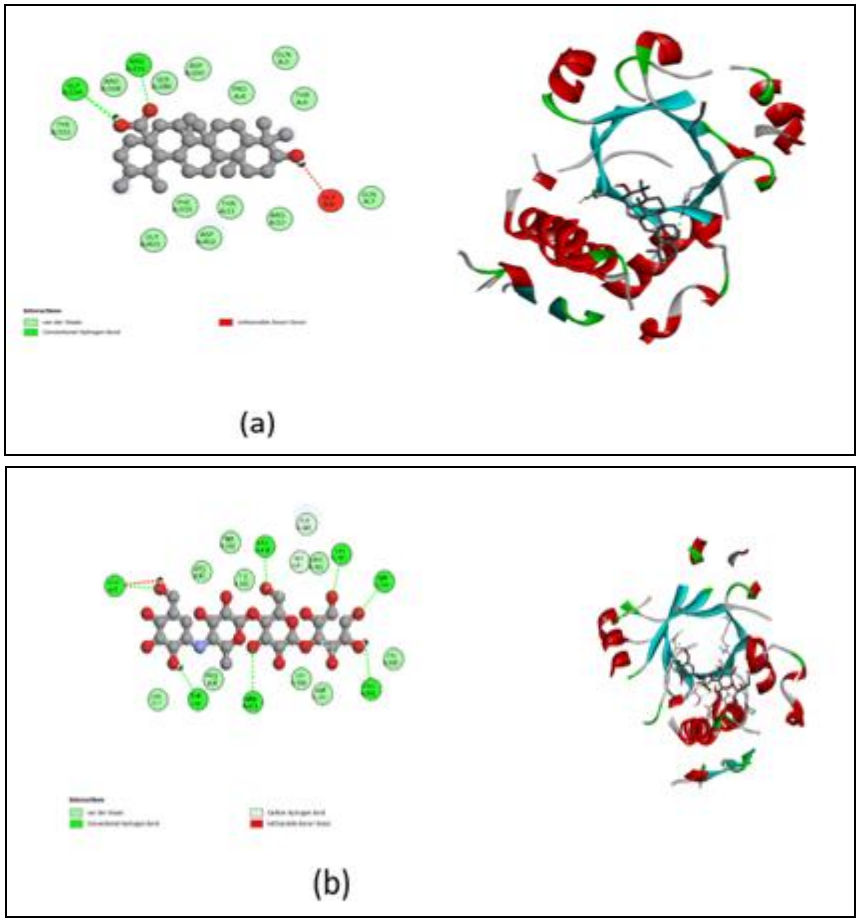

FIG. 10: MOLECULAR DOCKING INTERACTION DIAGRAMS OF URSOLIC ACID AND ACARBOSE WITH PORCINE PANCREATIC A-AMYLASE(PDB ID: 1OSE): (A) 2D INTERACTION MAP OF THE URSOLIC ACID–A-AMYLASE COMPLEX SHOWING HYDROGEN BONDING AND HYDROPHOBIC CONTACTS WITH KEY ACTIVE-SITE RESIDUES; (B) 3D BINDING POSE OF URSOLIC ACID WITHIN THE ENZYME ACTIVE SITE; (C) 2D INTERACTION MAP OF THE ACARBOSE–A-AMYLASE COMPLEX ILLUSTRATING EXTENSIVE HYDROGEN-BONDING INTERACTIONS; (D) 3D BINDING CONFORMATION OF ACARBOSE IN THE CATALYTIC POCKET.

CONCLUSION: Present study reports the systematic isolation and comprehensive structural characterization of ursolic acid from the leaves of *Eucalyptus tereticornis Sm*. using sequential Soxhlet extraction followed by column chromatographic purification. The identity and high purity (99.507%) of the isolate were unambiguously confirmed by an integrated suite of spectroscopic techniques, including FTIR, ^{1}H NMR, ^{13}C NMR, HPLC, and HRMS, all of which yielded data in close agreement with reported values for authentic ursolic acid. Biological evaluation demonstrated that the polar extracts of *E. tereticornis* particularly the methanol and acetone fractions possess potent antioxidant activity, with DPPH and ABTS IC_{50} values closely approaching those of the reference standards ascorbic acid and BHT. Similarly, these polar extracts exhibited significant α-amylase inhibitory activity, with IC_{50} values approximating that of the clinical standard acarbose. Although isolated ursolic acid showed moderate activity in all three bioassays, its activity was consistent across antioxidant and antidiabetic paradigms, indicating

intrinsic multifunctional pharmacological potential. Molecular docking analysis against porcine pancreatic α-amylase (PDB ID: 1OSE) revealed that ursolic acid binds within the enzyme's catalytic pocket with a competitive binding affinity of −7.5 kcal/mol, interacting with several key residues shared with the reference inhibitor acarbose (−8.6 kcal/mol). The predominantly hydrophobic mode of binding, augmented by selective hydrogen bonding, provides a mechanistic basis for the observed enzyme inhibition. *In-silico* ADMET profiling indicated that ursolic acid exhibits favorable drug-likeness (bioavailability score = 0.85, zero PAINS alerts, and no predicted CYP450 inhibition), albeit with limitations in aqueous solubility and gastrointestinal absorption, which may be amenable to structural optimization or formulation-based approaches. This investigation establishes *Eucalyptus tereticornissm.* as a scientifically validated natural source of ursolic acid and highlights the compound's promise as a multi-target phytochemical lead for the development of antioxidant and antidiabetic therapeutics. Future studies should focus on *in-vivo* pharmacological validation, nanoformulation-based bioavailability enhancement, and structure activity relationship studies to fully exploit the therapeutic potential of this triterpenoid scaffold.

ACKNOWLEDGEMENTS: The authors are thankful to the Director of CSIR–National Botanical Research Institute (CSIR-NBRI), Lucknow, India, for providing the necessary research facilities and support. The authors also acknowledge the University of Lucknow, Lucknow (226007), India, for Ph.D. registration (Registration No. 2010015346002) and academic support.

Declarations:

Author Contributions: S.C.: conceptualization, spectroscopy, writing — original draft. M.S.: biological assays, data curation. N.R.: supervision, writing — review & editing. All authors read and approved the final manuscript.

CONFLICT OF INTEREST: The authors declare no conflict of interest.

REFERENCES:

1. Babalola IT & Shode FO: Ubiquitous ursolic acid: a potential pentacyclic triterpene natural product. Journal of Pharmacognosy and Phytochemistry 2013; 2(2): 214–222.
2. Bishayee A, Ahmed S, Brankov N & Perloff M: Triterpenoids as potential agents for the chemoprevention and therapy of breast cancer. Frontiers in Bioscience 2011; 16(1): 980–1011. https://doi.org/10.2741/3730
3. Bhattacharya S: Reactive oxygen species and cellular defense system. In D. P. Bhattacharya (Ed.), Free Radicals in Human Health and Disease 2015; 17–29.
4. Checker R, Sandur SK, Sharma D, Patwardhan RS, Jayakumar S, Kohli V, Sethi G, Aggarwal BB & Sainis KB: Potent anti-inflammatory activity of ursolic acid, a triterpenoid antioxidant, is mediated through suppression of NF-κB, AP-1 and NF-AT. PLoS ONE 2012; 7(2): e31318. https://doi.org/10.1371/journal.pone.0031318
5. Kasabri V, Flatt PR & Abdel-Wahab YHA: Extracts of *Arctium lappa* and *Ceratonia siliqua* inhibit pancreatic amylase and glucosidase activity. Pharmaceutical Biology, 2010; 48(10): 1166–1172.
6. Derosa G & Maffioli P: α-Glucosidase inhibitors and their use in clinical practice. Archives of Medical Science 2012; 8(5): 899–906. https://doi.org/10.5114/aoms.2012.31621
7. Patil R & Patil R: Isolation of ursolic acid from Eucalyptus globulus and its antidiabetic activity. International Journal of Pharmaceutical Sciences and Research 2016; 7(3): 1127–1133.
8. Atanasov AG, Waltenberger B, Pferschy-Wenzig EM, Linder T, Wawrosch C, Uhrin P, Temml V, Wang L, Schwaiger S, Heiss EH, Rollinger JM, Schuster D, Breuss JM, Bochkov V, Mihovilovic MD, Kopp B, Bauer R, Dirsch VM & Stuppner H: Discovery and resupply of pharmacologically active plant-derived natural products: a review. Biotechnology Advances 2015; 33(8): 1582–1614. https://doi.org/10.1016/j.biotechadv.2015.08.001
9. Daina A, Michielin O & Zoete V: SwissADME: a free web tool to evaluate pharmacokinetics, drug-likeness and medicinal chemistry friendliness of small molecules. Scientific Reports 2017; 7: 42717. https://doi.org/10.1038/srep42717
10. Dhakad AK, Pandya V, Beg S, Rawat JM & Singh A: Biological, medicinal and toxicological significance of Eucalyptus leaf essential oil: a review. Journal of the Science of Food and Agriculture 2018; 98(3): 833–848. https://doi.org/10.1002/jsfa.8600
11. Li WQ, Wu XM, Xu MY & Ruan JL: Simultaneous determination of oleanolic acid and ursolic acid in Chinese medicinal herbs by HPLC. Journal of Liquid Chromatography & Related Technologies 2007; 30(13–14): 2015–2023.
12. Rao NB, Babu GDK, Kumar BR & Babu AVS: Isolation and characterization of ursolic acid from *Plumeria acutifolia*. International Journal of Pharmacy and Pharmaceutical Sciences 2010; 2(1): 76–78.
13. Jager S, Trojan H, Kopp T, Laszczyk MN & Scheffler A: Pentacyclic triterpene distribution in various plants—rich sources for a new group of multi-potent plant extracts. Molecules 2009; 14(6): 2016–2031. https://doi.org/10.3390/molecules14062016
14. Brand-Williams W, Cuvelier ME & Berset C: Use of a free radical method to evaluate antioxidant activity. LWT – Food Science and Technology 1995; 28(1): 25–30. https://doi.org/10.1016/S0023-6438(95)80008-5
15. Molyneux P: The use of the stable free radical diphenylpicrylhydrazyl (DPPH) for estimating antioxidant activity. Songklanakarin Journal of Science and Technology 2004; 26(2): 211–219.
16. Re R, Pellegrini N, Proteggente A, Pannala A, Yang M & Rice-Evans C: Antioxidant activity applying an improved ABTS radical cation decolorization assay. Free Radical

Biology and Medicine 1999; 26(9–10): 1231–1237. https://doi.org/10.1016/S0891-5849(98)00315-3
17. Pellegrini N, Re R, Yang M & Rice-Evans C: Screening of dietary carotenoids and carotenoid-rich fruit extracts for antioxidant activities applying 2,2′-azinobis(3-ethylenebenzothiazoline-6-sulfonic acid) radical cation decolorization assay. Methods in Enzymology 1999; 299: 379–389.
18. Bernfeld P: Amylases, α and β. Methods in Enzymology 1955; 1: 149–158. https://doi.org/10.1016/0076-6879(55)01021-5
19. Trott O & Olson AJ: AutoDock Vina: improving the speed and accuracy of docking with a new scoring function, efficient optimization, and multithreading. Journal of Computational Chemistry 2010; 31(2): 455–461. https://doi.org/10.1002/jcc.21334
20. Lipinski CA, Lombardo F, Dominy BW & Feeney PJ: Experimental and computational approaches to estimate solubility and permeability in drug discovery and development settings. Advanced Drug Delivery Reviews 2001; 46(1–3): 3–26. https://doi.org/10.1016/S0169-409X(00)00129-0
21. Savoia D: Plant-derived antimicrobial compounds: alternatives to antibiotics. Future Microbiology 2012; 7(8): 979–990.
22. Ikeda Y, Mori M, Yokota Y, Yanagisawa A, Yasuda I & Yonemitsu O: NMR spectral assignment of ursolic acid isolated from Sambucus nigra. Natural Product Letters 1999; 14(1): 15–21.
23. Szakiel A, Pączkowski C, Pensec F & Bertsch C: Fruit waxes as a source of biologically active triterpenoids. Phytochemistry Reviews 2012; 11(2–3): 263–284. https://doi.org/10.1007/s11101-012-9241-4
24. Gnoatto SCB, Dalla Vecchia R, De Souza MFV & Gosmann G: HPLC method for the determination of ursolic acid in Calendula officinalis L. crude extracts and fluid extract. Journal of the Brazilian Chemical Society 2008; 19(7): 1437–1441.
25. Silverstein RM, Webster FX, Kiemle DJ & Bryce DL: Spectrometric Identification of Organic Compounds (8th ed.). John Wiley & Sons 2014.
26. Szakiel A, Pączkowski C & Henry M: Influence of environmental abiotic factors on the content of saponins in plants. Phytochemistry Reviews 2011; 10(4): 471–491.
27. Prior RL, Wu X & Schaich K: Standardized methods for the determination of antioxidant capacity and phenolics in foods and dietary supplements. Journal of Agricultural and Food Chemistry 2005; 53(10), 4290–4302. https://doi.org/10.1021/jf0502698
28. Tundis R, Loizzo MR & Menichini F: Natural products as α-amylase and α-glucosidase inhibitors and their hypoglycaemic potential in the treatment of diabetes: an update. Mini-Reviews in Medicinal Chemistry 2010; 10(4): 315–331.
29. Mubashir K, Ganai BA, Ghazanfar K & Akbar S: Evaluation of *Hypericum perforatum* for its antidiabetic and antioxidant activities. International Scholarly Research Notices 2014; 450842.
30. Veber DF, Johnson SR, Cheng HY, Smith BR, Ward KW & Kopple KD: Molecular properties that influence the oral bioavailability of drug candidates. Journal of Medicinal Chemistry 2002; 45(12): 2615–2623. https://doi.org/10.1021/jm020017n
31. Sarpietro MG, Spatafora C, Tringali C, Micieli D & Castelli F: Interaction of ursolic acid and its O-acyl-derivative with DPPC membranes. European Journal of Pharmaceutical Sciences 2007; 30(5): 381–393.
32. Chaubey S, Rastogi N & Srivastava M: Exploring the medicinal potential of *Lantana camara*: a comprehensive review of phytochemicals and therapeutic application. Phytochem Rev 2026; 25: 23–53. https://doi.org/10.1007/s11101-025-10118-5
33. Maurya S and Anupam Tripathi S: Recent advances in the synthesis and applications of zinc oxide nanomaterials for healthcare energy and environmental systems. Discov Chem 2026; 3: 98. https://doi.org/10.1007/s44371-026-00570-3
34. Tiwari M, Pathan S, Sharma D, Chaubey S, Mishra V & Srivastava M: Secondary metabolites from plants. In Secondary Metabolites in Stress and Disease Management 2026; 3-25.

How to cite this article:
Chaubey S, Srivastava M and Rastogi N: Isolation of ursolic acid from leaves of *Eucalyptus tereticornis* smith: antioxidant, antidiabetic, molecular docking, and ADMET profiling. Int J Pharm Sci & Res 2026; 17(8): 2365-81. doi: 10.13040/IJPSR.0975-8232.17(8).2365-81.